

DOI: 10.1002/cbic.200900156

# Eosin Y-Sensitized Artificial Photosynthesis by Highly Efficient Visible-Light-Driven Regeneration of Nicotinamide Cofactor

Sahng Ha Lee,<sup>[a]</sup> Dong Heon Nam,<sup>[a]</sup> Jae Hong Kim,<sup>[a]</sup> Jin-Ook Baeg,<sup>[b]</sup> and Chan Beum Park<sup>\*,[a]</sup>

Mimicking natural photosynthesis is an attractive way to achieve a new form of renewable energy by using sunlight.<sup>[1]</sup> During the photosynthetic process, photon energy is absorbed by dye-sensitized photosystems and stored as chemical energy, which is then used for the synthesis of carbohydrates through the Calvin cycle. It is subsequently regenerated by a recycling process between light and dark reactions. For artificial photosynthesis, the photoinduced electron-transfer reaction should occur with a man-made light-harvesting antenna that can fulfil the role of both photosystems in natural photosynthesis. The efficient regeneration of nicotinamide or flavin cofactor is critical for the conversion of solar energy into fine chemicals because an oxidoreductase, working as a counterpart of the Calvin cycle, requires a stoichiometric amount of cofactors as redox equivalents.<sup>[2]</sup> Therefore, in order to develop an artificial photosynthetic system, it is important to identify an efficient means of photoinduced electron transfer, especially in the visible-light range.<sup>[3]</sup>

Herein we report a new self-assembled dyad for the visible-light-driven regeneration of a nicotinamide cofactor that involves Eosin Y (EY, 2,4,5,7-tetrabromofluorescein; Figure S1 in the Supporting Information), a dye photosensitizer. In the field of solar energy conversion, EY has been applied to the development of organic-inorganic hybrid dye-sensitized solar cells (DSSC),<sup>[4,5]</sup> and photocatalytic hydrogen production with the support of conductive matrices and platinum catalysts.<sup>[6,7]</sup> It is a promising photosensitizer that exhibits high quantum yields for DSSC devices, and its quantum efficiency for hydrogen evolution was reportedly much higher than other organic dyes, such as merocyanine and coumarin, when sensitized by visible light.<sup>[7]</sup>

We first employed the photoelectrochemical property of EY for the photoinduced electron-transfer reaction in an artificial photosynthetic process for L-glutamate synthesis, as illustrated in Figure 1A. The visible-light-driven electron-transfer reaction was conducted between EY and an electrochemical mediator,

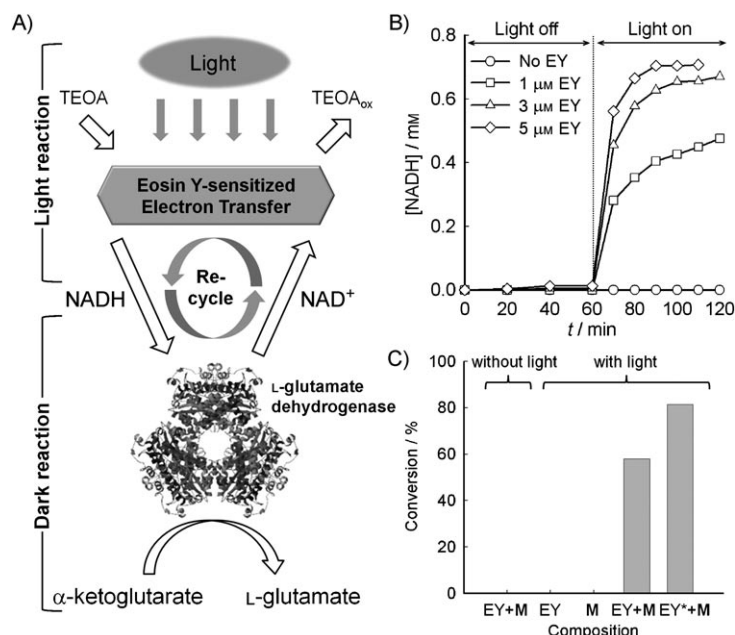


**Figure 1.** A) Schematic illustration of Eosin Y-sensitized artificial photosynthesis with L-glutamate dehydrogenase, B) photoregeneration of NADH (with 1 mM NAD<sup>+</sup>), and C) photoenzymatic synthesis of L-glutamate by glutamate dehydrogenase with Eosin Y concentrations of 10 μM (EY, EY + M) and 50 μM (EY\* + M), respectively.

(pentamethyl-cyclopentadienyl-2,2'-bipyridine-aqua) rhodium(III) (**M** = [Cp\*Rh(bpy)H<sub>2</sub>O]<sup>2+</sup>, Cp\* = C<sub>5</sub>Me<sub>5</sub>, bpy = 2,2'-bipyridine), for nonenzymatic NADH regeneration in the presence of a sacrificial electron donor, triethanolamine (TEOA). The organometallic compound, **M**, has been applied as a hydride transfer mediator for the indirect regeneration of NADH in chemical and electrochemical systems due to its high selectivity for the regeneration of enzymatically active cofactors.<sup>[8]</sup> Unlike other mediators like methyl viologen, **M** is nontoxic for enzymes and it does not require a secondary enzyme for selective regeneration of enzymatically active cofactor.<sup>[8d]</sup>

According to our analysis, NAD<sup>+</sup> was not reduced to NADH at all in the dark stage, whereas irradiation with visible light of the same reaction medium triggered rapid NADH generation (Figure 1B). In the visible-light-induced NADH regeneration that was carried out with various concentrations of EY and 0.25 mM **M**, the rate of photocatalytic NADH reduction was proportional to the concentration of EY, and the reaction reached its maximum yield (71 %) within 30 min of light irradiation with 5 μM EY. The initial turnover frequency for NADH regeneration was estimated to be 1690 h<sup>-1</sup> with 1 μM EY. We further performed EY-sensitized enzymatic photosynthesis of L-glutamate by glutamate dehydrogenase (Figure 1C). A control experiment that was conducted in the absence of light result-

[a] S. H. Lee, D. H. Nam, J. H. Kim, Prof. C. B. Park  
Department of Materials Science and Engineering  
Korea Advanced Institute of Science and Technology  
373-1 Guseong-dong, Yuseong-gu, Daejeon 305-701 (Korea)  
Fax: (+82)42-350-3310  
E-mail: parkcb@kaist.ac.kr

[b] Dr. J.-O. Baeg  
Advanced Chemical Technology Division  
Korea Research Institute of Chemical Technology (KRICT)  
100 Jang-dong, Yuseong-gu, Daejeon 305-343 (Korea)

Supporting information for this article is available on the WWW under <http://dx.doi.org/10.1002/cbic.200900156>.

ed in a null yield of L-glutamate. It is notable that L-glutamate was not produced without **M**; this indicates the critical role of **M** in the photoenzymatic synthesis. In addition, **M** alone (i.e., without EY) was not photoactive, and no conversion was observed for the single-mediator system. When the both mediators, that is, EY and **M** were present together, yields of 57.9 and 81.4% were obtained after 40 min of reaction with EY concentrations of 10  $\mu\text{M}$  (EY + **M**) and 50  $\mu\text{M}$  (EY\* + **M**), respectively. Prolonged (80 min) reactions resulted in the maximum conversions of approximately 90% in both experiments. Figure 2A shows the turnover frequency of EY in the photoenzymatic synthesis of L-glutamate compared to previously reported organic, organometallic, and semiconductor sensitizers. The turnover frequency of EY was 15 times higher than Ru(bpy)<sub>3</sub> and 382 times higher than PEG-chlorophyllide. Also, the turnover number of NAD(P)<sup>+</sup> (Figure 2B) was estimated to be at least ten times higher in the EY-sensitized photoenzymatic system.<sup>[3,9]</sup>

The superior performance of EY in the photoenzymatic synthesis is attributed to its complexation with **M** that was observed to guide the excited electrons of EY to the catalytic center of **M**. To investigate the interaction between EY and **M**, we observed the spectral changes of EY absorbance in the presence of **M** under various concentrations at pH 7.0. According to our observation, the onset and peak of EY absorption red-shifted with the increasing concentration of **M** (Figure 3A). We attribute the pH-independent absorbance change in Figure 3A to the molecular interaction between EY and **M** by the binding of carboxyl group of EY with the metal center of **M**. The carboxyl group of EY is known to form complexes with metal ions like Zn<sup>2+</sup>.<sup>[10]</sup> Previously, EY was reported to undergo the red-shift of absorbance with decreasing pH by the change in the ionization state (that is, protonation) of EY's carboxyl group.<sup>[11]</sup>

We also observed the red-shift of emission maximum and the decrease of EY's fluorescence intensity when the concentration of **M** was increased (Figure 3B). According to Moser and Grätzel,<sup>[11]</sup> the emission spectrum of EY red-shifted because of the polarizability and electronegativity of metal cations when bound to metallic materials, such as TiO<sub>2</sub>. The decrease of emission intensity in Figure 3B implies that the radiative decay of excited electrons was inhibited by **M**. The excited electrons of EY were reported to be transferred to the conduction band of matrix materials, such as semiconducting oxide nanoparticles (for example, ZrO<sub>2</sub>, Al<sub>2</sub>O<sub>3</sub>, TiO<sub>2</sub>), with quenched fluorescence when adsorbed onto the surface of matrices.<sup>[12]</sup> We further confirmed the formation of the EY–**M** complex by using FTIR analysis (Figure S2), which shows that the Rh–O bond in **M** was changed from H<sub>2</sub>O to EY.

We further examined the electrochemical properties of EY and **M** with cyclic voltammetry (CV) and

linear sweep voltammetry (LSV) by using a glassy carbon electrode at pH 7.0 in a phosphate buffer (100 mM). The reduction peak potential of **M** was estimated at –0.70 V and a reductive current of EY resulted from –1.0 V in a solution that only contained EY (Figure 4A). The CV voltammogram changed when the two components were present in solution; the reduction of mixture was observed at –0.75 V with a cathodic shift of **M**

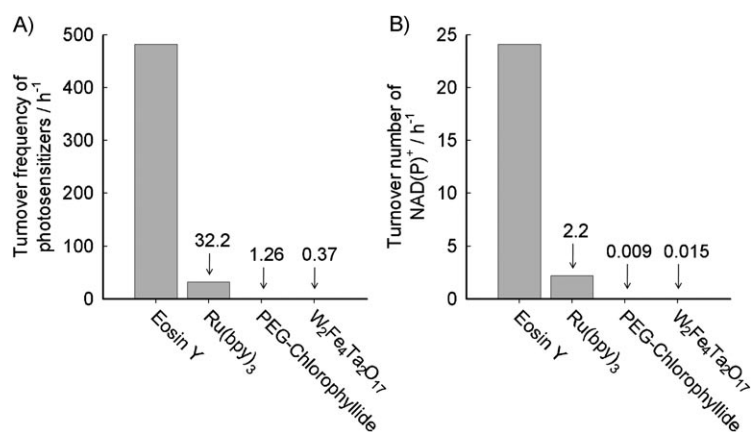


**Figure 2.** Performance of Eosin Y-sensitized visible-light driven enzymatic synthesis of L-glutamate compared to previous reports (Ru(bpy)<sub>3</sub>,<sup>[9a]</sup> PEG-chlorophyllide,<sup>[9b]</sup> W<sub>2</sub>Fe<sub>4</sub>Ta<sub>2</sub>O<sub>17</sub>)<sup>[3]</sup> in terms of A) photosensitizer turnover frequency and B) NAD(P)<sup>+</sup> turnover number. For detailed information about reaction conditions, please refer to the Supporting Information.

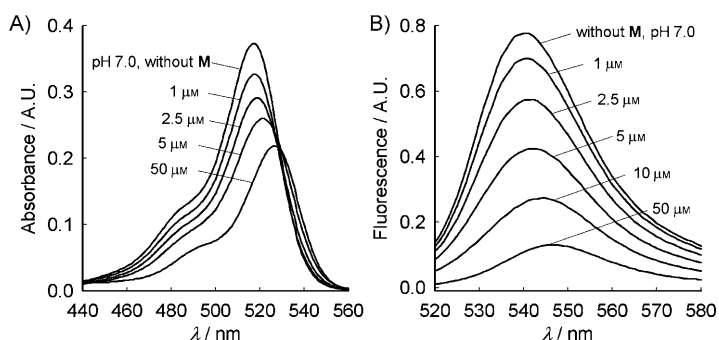


**Figure 3.** The change in A) absorbance and B) fluorescence of Eosin Y (5  $\mu\text{M}$ ) in the presence of **M** in various concentrations.

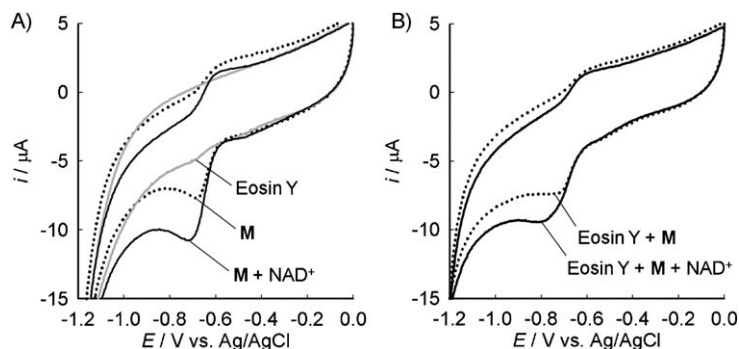


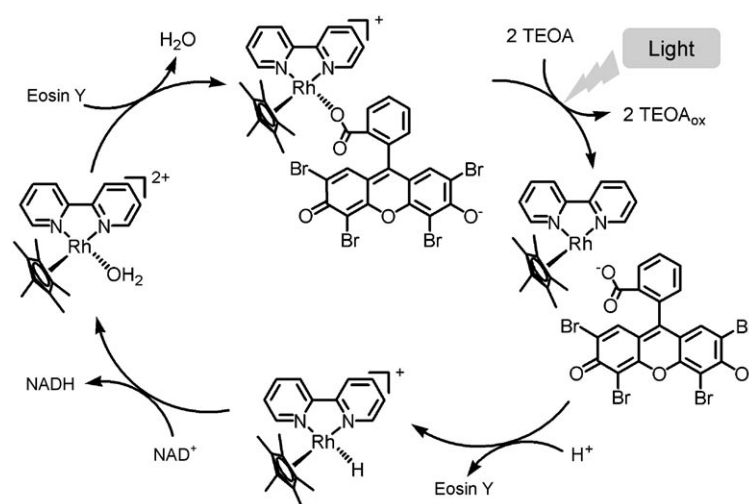
**Figure 4.** Cyclic voltammograms of A) **M** (250  $\mu\text{M}$ ) and Eosin Y (50  $\mu\text{M}$ ) solutions and B) mixture of two components in the presence and absence of NAD<sup>+</sup> (1 mM). The potential was scanned at 100 mV s<sup>-1</sup>.

reduction, which can be also interpreted as an anodic shift of EY reduction (Figure 4B). Results of LSV experiments showed substantial changes in the reduction peak potentials of EY and **M** (Figure S3). These results suggest a coreduction reaction of EY and **M** through the intermediate EY–**M** complex. According to a previous report,<sup>[4]</sup> the co-reduction reaction occurred with an anodic shift in the CV voltammogram when EY and a stabilizing component, such as  $\text{Zn}(\text{NO}_3)_2$ , were present in a solution.

To confirm the catalytic interaction between the EY–**M** complex and  $\text{NAD}^+$ , the voltammetric measurements were performed in the presence of  $\text{NAD}^+$ . As shown in Figure 4A, the catalytic effect of **M** results in the strongly increased rate of **M** reduction in the presence of  $\text{NAD}^+$ . The EY–**M** complex also exhibited a strong increase in reduction peak current with  $\text{NAD}^+$ , implying a mediation system that consisted of EY and **M** was able to catalyze the reduction of  $\text{NAD}^+$  (Figure 4B). The absence of oxidation peak indicates that the EY–**M** complex follows the electrochemistry of **M** (i.e., two-electron reduction followed by chemical protonation). As an electron acceptor in the complex, **M** also suppressed the reduction and oxidation peaks of EY appearing on an Au electrode (Figure S4).

The photoelectrical behavior of EY should account for the catalytic activity of the EY–**M** complex because the excited electron of EY could be easily transferred to **M**. According to Goux et al.,<sup>[10]</sup> the photoelectrical property of EY in the hybrid DSSC comes from the excitation of electrons from HOMO to LUMO in EY, followed by the transfer of the excited electrons onto the conduction band of semiconducting matrices. Once the electron of EY at the known HOMO (1.09 V)<sup>[6]</sup> is excited to the LUMO (−1.02 V, from Figure S3), it should cascade into **M** through the intermediate state of EY–**M** without radiation (e.g., fluorescence) as illustrated in Figure S5. The successive transfer of electrons from TEOA to EY should result in the electrical reduction of **M**. The electrically reduced **M**,  $[\text{Cp}^*\text{Rh}(\text{bpy})]$ , would be chemically protonated in aqueous media, followed by its catalytic reaction with  $\text{NAD}^+$ . Based on our results, we suggest that EY and **M** form a coupled intermediate to transfer electrons to  $\text{NAD}^+$ , as illustrated in Scheme 1. During the photoinduced electron transfer cycle, EY and **M** were reversibly bound together through the metal center of **M** ( $\text{Rh}^{2+}$ ) and the ionized carboxyl group of EY. The vicinity and potential gradient between the photosensitizer (EY) and the electrocatalytic center (**M**) enabled an efficient transfer of electrons to regenerate  $\text{NADH}$  with high turnover rate and frequency.

In summary, EY was first introduced as a molecular photosensitizer for visible-light-driven regeneration of  $\text{NADH}$  in the presence of **M** and sacrificial electron donor. An efficient regeneration of  $\text{NADH}$  with a high turnover rate was achieved through a new photosensitizer–electron relay dyad (EY–**M**) whose components bound to each other. Photochemical regeneration of the nicotinamide cofactor, coupled with enzymatic reaction catalyzed by glutamate dehydrogenase, was



**Scheme 1.** The catalytic cycle of **M** during the Eosin Y-sensitized, nonenzymatic photochemical regeneration of  $\text{NADH}$  involving two electron-transfer reaction between **M** and Eosin Y.

successfully conducted as a model dye-sensitized artificial photosynthetic system.

## Experimental Section

**Materials:** All chemicals, including EY, TEOA, and  $\text{NAD}^+$ , were purchased from Sigma–Aldrich in the purity over reagent grade and were used without further purification. EY (1 mM) was dissolved in deionized  $\text{H}_2\text{O}$  and used as a stock solution for all experiments.

**Synthesis of  $[\text{Cp}^*\text{Rh}(\text{bpy})\text{Cl}]\text{Cl}$ :** The hydridorhodium complex, **M**, was synthesized by the method of Kölle and Grätzel (Figure S6). A mixture of  $\text{RhCl}_3 \cdot 3\text{H}_2\text{O}$  (200 mg) and hexamethyldewarbenzen (HMDB, 40 mg) in MeOH (6 mL) was stirred at 65 °C under  $\text{N}_2$  for 15 h. The mixture was allowed to cool to room temperature, and the solvent was removed under vacuum. The residue was washed with  $\text{Et}_2\text{O}$  to remove excess hexamethylbenzene; this left oily red crystals, which were extracted with  $\text{CHCl}_3$ . The solution was dried over anhydrous  $\text{MgSO}_4$ , evaporated under reduced pressure, and the residue was recrystallized from  $\text{CHCl}_3$ /benzene. Upon addition of 2,2'-bipyridine (2 equiv), the suspension cleared almost immediately, and a yellowish solution was formed. From this sample,  $[\text{Cp}^*\text{Rh}(\text{bpy})\text{Cl}]\text{Cl}$  was precipitated upon the addition of  $\text{Et}_2\text{O}$ . Yield: 120 mg (70%, based on compound 1).  $^1\text{H}$  NMR (300 MHz,  $\text{CDCl}_3$ ):  $\delta$  = 9.11 (d, 2H; H-3,3'), 8.84 (d, 2H; H-6,6'), 8.27 (t, 2H; H-5,5'), 7.81 (t, 2H; H-4,4'), 1.75 ppm (s, 15H, Cp\*); the spectrum is shown in Figure S7.

**Photochemical reaction:** The photochemical regeneration of  $\text{NADH}$  was performed within a quartz reactor under an argon atmosphere at room temperature. A 400 W W-halogen lamp equipped with a 420 nm cut-off filter was used as a light source. Eosin Y-sensitized photoregeneration of  $\text{NADH}$  was carried out as follow: After 1 h of incubation without light (light-off), the reactor was exposed to light (light-on) at pH 7.0. The reactor was composed of  $\text{NAD}^+$  (1 mM), **M** (0.25 mM), TEOA (15% w/v), and phosphate buffer (100 mM) with different concentrations of EY. The photoenzymatic reactors for photosynthesis of L-glutamate were composed of Eosin Y (10  $\mu\text{M}$  for EY and 50  $\mu\text{M}$  for EY\*), **M** (0.5 mM),  $\text{NAD}^+$  (0.2 mM),  $\alpha$ -ketoglutarate (5 mM), ammonium sulfate

(100 mM), and glutamate dehydrogenase (40 U), based on a phosphate buffer (100 mM), with TEOA (15% w/v; pH 8.0). Reactions were carried out under varied conditions, including the absence of **M** or EY.

**Analysis:** Spectrophotometric and spectrofluorometric experiments were performed with the BioSpec-mini (Shimadzu Co., Japan) and RF-5301PC (Shimadzu Co., Japan), respectively. In both measurements, Eosin Y (5  $\mu$ M) was used with various concentrations of **M**. The fluorescence spectra were obtained with excitation wavelength of 400 nm. Voltammetric experiments were performed with a single-cell compartment configured with a 3-electrode system: a glassy carbon or Au disk (working diameter 2 mm), a platinum wire (counter) and an Ag/AgCl<sub>sat'd</sub> KCl (reference, 0.197 V versus normal hydrogen electrode) connected to a potentiostat/galvanostat (EG&G, model 263 A). **M** (0.25 mM), Eosin Y (50  $\mu$ M) and NAD<sup>+</sup> (1 mM) were used in a phosphate buffer (100 mM) at pH 7.0. The concentration of NADH was measured spectrophotometrically through its absorbance at 340 nm. High-performance liquid chromatography (LC-20A prominence, Shimadzu Co.), equipped with an Inertsil C<sub>18</sub> column (ODS-3V, length, 150 mm), was used for the analysis of enzymatic reactions. Samples were eluted by phosphoric acid (0.085%) with flow rate of 1.0 mL min<sup>-1</sup> and detected at 210 nm. The FTIR spectra were obtained with a FTIR microscope (IFS 66v/s, Bruker Optics). Samples were spread on Au-coated substrates and dried overnight before measurement.

## Acknowledgements

This work was supported by Korea Science and Engineering Foundation (KOSEF) National Research Laboratory (ROA-2008-000-20041-0) and Engineering Research Center (R11-2008-058-03003-0) Programs, and the High Risk High Return Project from the office of KAIST, Republic of Korea.

**Keywords:** biocatalysis • Eosin Y • NADH regeneration • photosynthesis • redox enzymes

- [1] a) J. H. Alstrum-Acevedo, M. K. Brennaman, T. J. Meyer, *Inorg. Chem.* **2005**, *44*, 6802–6827; b) L. Hammarström, *Curr. Opin. Chem. Biol.* **2003**, *7*, 666–673.
- [2] a) R. Devaux-Basseguy, A. Bergel, M. Comtat, *Enzyme Microb. Technol.* **1997**, *20*, 248–258; b) H. Zhao, W. A. van der Donk, *Curr. Opin. Biotechnol.* **2003**, *14*, 583–589; c) A. Taglieber, F. Schulz, F. Hollmann, M. Rusek, M. T. Reetz, *ChemBioChem* **2008**, *9*, 565–572.
- [3] C. B. Park, S. H. Lee, E. Subramaniam, B. B. Kale, S. M. Lee, J. O. Baeg, *Chem. Commun. (Cambridge)* **2008**, 5423–5425.
- [4] T. Yoshida, K. Terada, D. Schlettwein, T. Oekermann, T. Sugiura, H. Minoura, *Adv. Mater.* **2000**, *12*, 1214–1217.
- [5] S.-S. Kim, J.-H. Yum, Y.-E. Sung, *Sol. Energy Mater. Sol. Cells* **2003**, *79*, 495–505.
- [6] R. Abe, K. Hara, K. Sayama, K. Domen, H. Arakawa, *J. Photochem. Photobiol. A* **2000**, *137*, 63–69.
- [7] Q. Li, L. Chen, G. Lu, *J. Phys. Chem. C* **2007**, *111*, 11494–11499.
- [8] a) U. Kölle, S. S. Kang, P. Infelta, P. Comte, M. Grätzel, *Chem. Ber.* **1989**, *122*, 1869–1880; b) E. Steckhan, S. Hermann, R. Ruppert, E. Dietz, M. Frede, E. Spika, *Organometallics* **1991**, *10*, 1568–1577; c) H. C. Lo, C. Leiva, O. Buriez, J. B. Kerr, M. M. Olmstead, R. H. Fish, *Inorg. Chem.* **2001**, *40*, 6705–6716; d) F. Hollmann, B. Witholt, A. Schmid, *J. Mol. Catal. B* **2002**, *19*, 167–176; e) H. K. Song, S. H. Lee, K. Won, J. H. Park, J. K. Kim, H. Lee, S. J. Moon, D. K. Kim, C. B. Park, *Angew. Chem.* **2008**, *120*, 1773–1776; *Angew. Chem. Int. Ed.* **2008**, *47*, 1749–1752.
- [9] a) D. Mandler, I. Willner, *J. Chem. Soc. Perkin Trans. 2* **1986**, 805–811; b) H. Asada, T. Itoh, Y. Kodera, A. Matsushima, M. Hiroto, H. Nishimura, Y. Inada, *Biotechnol. Bioeng.* **2001**, *76*, 86–90.
- [10] A. Goux, T. Pauporté, D. Lincot, L. Dunsch, *ChemPhysChem* **2007**, *8*, 926–931.
- [11] J. Moser, M. Grätzel, *J. Am. Chem. Soc.* **1984**, *106*, 6557–6564.
- [12] S. Pelet, M. Grätzel, J. E. Moser, *J. Phys. Chem. B* **2003**, *107*, 3215–3224.

Received: March 19, 2009

Published online on June 23, 2009